Hydrogenases

Deutsche Ausgabe: DOI: 10.1002/ange.201507022
Internationale Ausgabe: DOI: 10.1002/anie.201507022

A High-Valent Iron(IV) Peroxo Core Derived from O_2

*Takahiro Kishima, Takahiro Matsumoto, Hidetaka Nakai, Shinya Hayami, Takehiro Ohta, and Seiji Ogo**

Abstract: *Dioxygen-tolerant [NiFe] hydrogenases catalyze not only the conversion of H_2 into $2H^+$ and $2e^-$ but also the reduction of O_2 to H_2O. Chemists have sought to mimic such bifunctional catalysts with structurally simpler compounds to facilitate analysis and improvement. Herein, we report a new [NiFe]-based catalyst for O_2 reduction via an O_2 adduct. Structural investigations reveal the first example of a side-on iron(IV) peroxo complex.*

Dioxygen-tolerant [NiFe] hydrogenases are bifunctional enzymes that act as both oxidases and hydrogenases.[1–5] We have previously reported a bifunctional model compound, based on a [NiRu] core, that is capable of switching from H_2 oxidation to O_2 reduction by replacing an η^6-C_6Me_6 ligand with an η^5-C_5Me_5 ligand.[6,7] Although we previously reported an H_2-oxidizing [NiFe] complex,[4] it was not capable of also reducing O_2. We have now developed this catalyst into a mimic of O_2-tolerant [NiFe] hydrogenases with the ability to reduce O_2 depending on the ligands. The previously reported H_2-oxidizing catalyst bears three electron-withdrawing $P(OEt)_3$ ligands, but replacing these ligands with an even stronger electron-donating η^5-C_5Me_5 ligand results in O_2 reduction. We have confirmed that the reaction proceeds via a side-on Fe^{IV} peroxo species $[Ni^{II}LFe^{IV}(\eta^2\text{-}O_2)(\eta^5\text{-}C_5Me_5)]^+$ (**2**, L = *N*,*N*′-diethyl-3,7-diazanonane-1,9-dithiolato; Figure 1), which accepts four electrons and four protons to generate two molecules of H_2O.

The solvent-coordinated complexes $[Ni^{II}LFe^{II}(RCN)(\eta^5\text{-}C_5Me_5)]^+$ (**1a**: R = Et, **1b**: R = Me; see the Supporting Information, Figure S1) were synthesized from the reaction of the nickel complex $[Ni^{II}L]$ and the iron complex $[Fe^{II}(MeCN)(CO)_2(\eta^5\text{-}C_5Me_5)]^+$. X-ray analysis of **1a** and **1b** revealed that the Ni and Fe atoms are tethered by the thiolato units of L, which results in the butterfly NiFe cores (Figure S2, Table S1). The interatomic distance between the Ni and Fe atoms [3.2325(6) Å] and the Ni-S-Fe angles [92.93(2)° and 93.25(2)°] of **1a** are comparable to those of **1b** [Ni···Fe: 3.2407(7) Å, Ni-S-Fe: 93.35(3)° and 93.40(2)°]. The Mössbauer spectrum of **1a** at 5 K in the absence of a magnetic field shows an isomer shift (δ) of 0.55 mm s^{-1} and a quadrupole splitting (ΔE_Q) of 2.1 mm s^{-1} (Figure S3), which is typical of the low-spin d^6 state found in ferrocene derivatives.[8] Complexes **1a** and **1b** are diamagnetic as confirmed by their ^{1}H NMR spectra (Figure S4) and the ESR silence at 128 K. Complexes **1a** and **1b** were then characterized by IR spectroscopy (Figure S5) and positive-ion electrospray ionization (ESI) mass spectrometry (Figure S6).

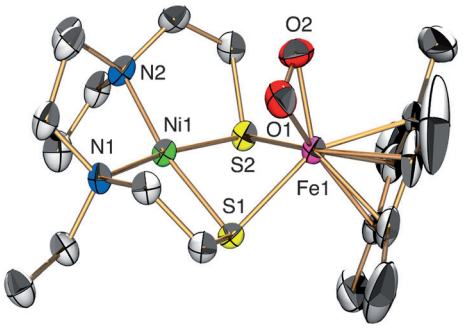

Figure 1. ORTEP drawing of **2**-BPh_4 with ellipsoids set at the 50% probability level. The counteranion (BPh_4), solvent (diethyl ether), and hydrogen atoms are omitted for clarity. Selected interatomic distances [Å] and angles [°]: Ni1···Fe1 3.0354(7), Fe1–O1 1.904(2), Fe1–O2 1.890(2), O1–O2 1.381(3); Ni1-S1-Fe1 85.84(3), Ni1-S2-Fe1 85.16(3), Fe1-O1-O2 68.11(14), Fe1-O2-O1 69.22(13), O1-Fe1-O2 42.67(10).

Complexes **1a** and **1b** are unreactive towards H_2 but reactive towards O_2 to form an O_2 adduct **2** (Figure S1). Bubbling O_2 through a propionitrile solution of **1a** at −80 °C or an acetonitrile solution of **1b** at −40 °C induced color changes from purple to brown, indicative of the formation of **2**. The UV/Vis spectrum of **2** shows charge-transfer bands at 410 nm ($\varepsilon = 3000\,M^{-1}cm^{-1}$) and 520 nm ($\varepsilon = 1500\,M^{-1}cm^{-1}$; Figure S7, Table S1). Formation of the O_2 adduct **2** is irreversible, which is not perturbed by an N_2 or H_2 purge.

The O_2 adduct **2** was recrystallized from an acetonitrile/diethyl ether solution to afford dark brown crystals suitable for X-ray analysis. The resulting diffraction pattern conclusively demonstrated the formation of an Fe–O_2 complex, where the O_2 ligand is bound to the Fe center in an η^2-fashion.[9–17] Notably, the O–O bond length of 1.381(3) Å is

[*] T. Kishima, Dr. T. Matsumoto, Dr. H. Nakai, Prof. S. Ogo
Center for Small Molecule Energy
Department of Chemistry and Biochemistry
Graduate School of Engineering
Kyushu University
744 Moto-oka, Nishi-ku, Fukuoka 819-0395 (Japan)
ogo.seiji.872m.kyushu-u.ac.jp
Homepage: http://www.cstm.kyushu-u.ac.jp/ogo/
Dr. T. Matsumoto, Dr. H. Nakai, Prof. S. Ogo
International Institute for Carbon-Neutral Energy Research (WPI-I2CNER), Kyushu University
744 Moto-oka, Nishi-ku, Fukuoka 819-0395 (Japan)
Prof. S. Hayami
Graduate School of Science and Technology
Kumamoto University
2-39-1 Kurokami, Chuo-ku, Kumamoto 860-8555 (Japan)
Dr. T. Ohta
Institute for Materials Chemistry and Engineering
Kyushu University
Higashi-ku, Fukuoka 812-8581 (Japan)

Supporting information for this article is available on the WWW under http://dx.doi.org/10.1002/anie.201507022.

within the region typical for side-on metal peroxo complexes (metal = Cu^{III} or Ni^{III})[18–20] and similar to that of biological side-on Fe^{III} peroxo species found in naphthalene dioxygenase (1.4 Å).[17] The bond is longer, however, than those in synthetic side-on Fe^{III} superoxo complexes [1.306(7)–1.323(3) Å][14] or biological side-on superoxo Fe^{II} species, found, for example, in homoprotocatechuate 2,3-dioxygenase (1.34 Å)[15] and homogentisate 1,2-dioxygenase (1.35 Å).[16] In the O_2 adduct, the distance between the Ni and Fe atoms [3.0354(7) Å] is significantly shorter than in the free complexes **1a** and **1b**.

Complex **1a** was then exposed to O_2 at −80 °C to perform kinetic studies. The reaction was carried out in O_2-saturated propionitrile and obeyed pseudo-first-order kinetics with respect to **1a** over five half-lives, as monitored by UV/Vis spectroscopy. The rate constant (k_{obs}) was determined to be 6.0×10^{-4} s^{-1} (Figure S7).

The positive-ion ESI mass spectrum of **2** in propionitrile shows a prominent signal at *m*/*z* 529.1 (relative intensity = 100 % in the range of *m*/*z* 100–2000), which corresponds to $[\mathbf{2}]^+$, and a characteristic isotopic distribution that matches well with the calculated one (Figure S8). To establish the origin of the peroxo ligand in **2**, $[Ni^{II}LFe^{IV}(\eta^2\text{-}^{18}O_2)(\eta^5\text{-}C_5Me_5)]^+$ (^{18}O-labeled **2**) was synthesized by the reaction of **1a** with $^{18}O_2$ in propionitrile. The ESI-MS results show that the signal at *m*/*z* 529.1 was shifted to 533.1, which demonstrates that the peroxo ligand was derived from dioxygen.

The IR spectrum of **2** in the solid state at −100 °C shows an isotope-sensitive band at 940 cm^{-1}, which was assigned to the O–O stretching vibration (Figure 2). Isotopic substitution

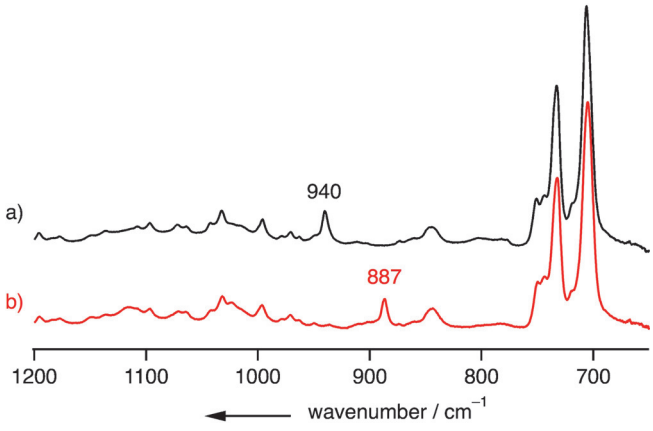

Figure 2. IR spectra of a) **2**-BPh_4 and b) ^{18}O-labeled **2**-BPh_4 in the solid state at −100 °C.

of $^{16}O_2$ by $^{18}O_2$ in the peroxo ligand (^{18}O-labeled **2**) resulted in a band shift to 887 cm^{-1}. The magnitude of the shift (53 cm^{-1}) agrees well with that expected by a calculation for a pure O_2 stretching mode according to Hooke's law. The wavenumber of the O–O stretching vibration is typical for side-on metal peroxo complexes (metal = Cu^{III} or Ni^{III}).[18–20] Alternatively, ^{18}O-labeled **2** could be synthesized from ^{16}O-labeled **2** with 500 equivalents of $H_2{}^{18}O_2$ in CH_3CN at −40 °C [Eq. (1)] and vice versa (Figure S9).

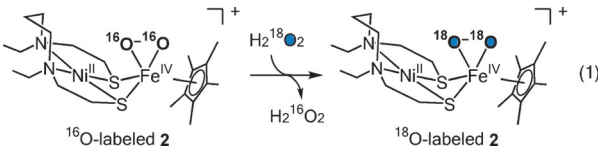

The ^{57}Fe Mössbauer spectrum of **2** at 30 K in the absence of a magnetic field shows an isomer shift (δ) of 0.42 mm s^{-1} and a quadrupole doublet (ΔE_Q) of 0.33 mm s^{-1} (Figure S10), suggesting an Fe^{IV} state. These values are close to those of $[Fe^{IV}(O)(H_2O)_5]^{2+}$ ($\delta = 0.38$ mm s^{-1}, $\Delta E_Q = 0.33$ mm s^{-1}).[21] The O–O bond length, IR spectroscopy, and $H_2{}^{18}O_2$ experiments indicate that the oxidation state of Fe in **2** is +4. For confirmation, the magnetic susceptibility was investigated by using a superconducting quantum interference device (SQUID) magnetometer. A solid sample of **2** was analyzed over a temperature range of 5–200 K, which revealed a magnetic moment of $S = 0$ in the ground state. The diamagnetic nature of **2** ($S = 0$) was corroborated by the signals in the diamagnetic region of the ^{1}H NMR spectrum (Figure S11).

Complex **2** is capable of reducing the coordinated peroxide to H_2O by supplying additional electrons and protons, as shown by an ^{18}O isotope-labeling experiment with **1b**. This complex reacted with an excess of $^{18}O_2$ in the presence of BH_4^- as the electron source and ethanol as the proton source in acetonitrile, which yielded $H_2{}^{18}O$ with a turnover number (TON) of 1.3 according to GC-MS analysis (Figure S12). We also confirmed that ^{18}O-labeled **2** produced $H_2{}^{18}O$ in the presence of BH_4^- and ethanol under stoichiometric conditions [Eq. (2)].

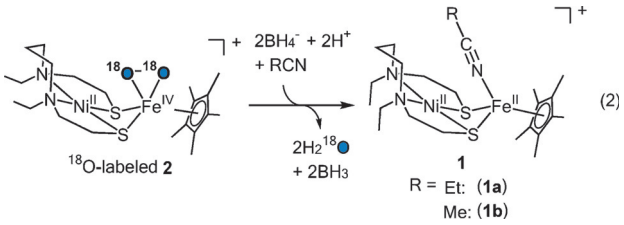

We also investigated the reduction of O_2 by cyclic voltammetry (CV) and rotating-disk electrode (RDE) voltammetry at several rotation rates (Figures S13 and S14). Based on the slope of the Koutecky–Levich plot, the number of electrons needed to reduce O_2 was determined to be 4.0.

Based on these results, we propose a catalytic cycle for O_2 activation by our O_2-tolerant [NiFe] hydrogenase model (Figure 3). Exposure of **1** to O_2 generates the oxygenated species **2**, which is further reduced by four additional electrons and four protons supplied from the electron and proton sources to regenerate **1**.

In conclusion, we have synthesized and characterized a catalyst for O_2 activation and proposed its use as a model for studying O_2-tolerant [NiFe] hydrogenases. A remarkable property of this catalyst is that the intermediate is based on a side-on iron(IV) peroxo core.

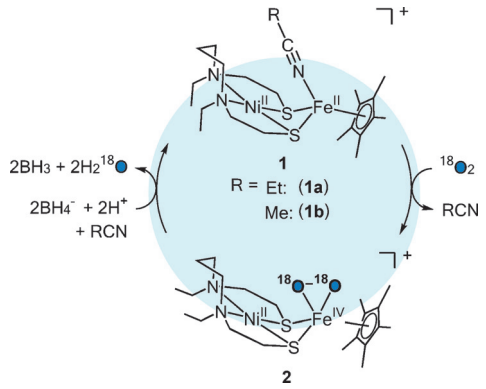

Figure 3. Activation of O_2 by a [NiFe] complex. The formation of $H_2{}^{18}O$ was confirmed by an isotope-labeling experiment using $^{18}O_2$.

Experimental Section

$[Ni^{II}LFe^{IV}(\eta^2\text{-}O_2)(\eta^5\text{-}C_5Me_5)]BPh_4$ (**2**-BPh_4): A propionitrile solution (4.0 mL) of **1a**-BPh_4 (50 mg, 57 μmol) was gradually layered with diethyl ether (100 mL) under an N_2 atmosphere. The resulting solution was cooled to −80 °C; it was then allowed to stand under an O_2 atmosphere to form a brown precipitate of thermally unstable **2**-BPh_4, which was collected by filtration, washed with cold diethyl ether, and dried in vacuo at −80 °C (31 % yield based on **1a**-BPh_4, estimated by the weight of the decomposed product(s)). Complex **2** is stable for 90 min at −40 °C and for one week at −80 °C. ^{1}H NMR (300 MHz, [D5]propionitrile, referenced to TMS, −80 °C): $\delta = 1.02$ (t, 6H, NCH_2CH_3), 1.50 (s, 15H, $C_5(CH_3)_5$), 1.94–4.61 (m, 18H, CH_2), 8.58–9.04 ppm ($B(C_6H_5)_4$). ESI-MS (in propionitrile): *m*/*z* 529.1 ($[\mathbf{2}]^+$, relative intensity (*I*) = 100 % in the range of *m*/*z* 100–2000). FT-IR (solid state at −100 °C): 940 cm^{-1} (O–O). Mössbauer (solid sample at 30 K in the absence of a magnetic field): $\delta = 0.42$, $\Delta E_Q = 0.33$.

$[Ni^{II}LFe^{IV}(\eta^2\text{-}{}^{18}O_2)(\eta^5\text{-}C_5Me_5)]BPh_4$ ($[^{18}O_2]$-**2**-BPh_4) was prepared by the same method as **2**-BPh_4 except for that $^{18}O_2$ was used instead of O_2. ESI-MS (in propionitrile): *m*/*z* 533.1 ($[[^{18}O_2]\text{-}\mathbf{2}]^+$, $I = 100$ % in the range of *m*/*z* 100–2000). FT-IR (solid state at −100 °C): 887 cm^{-1} (^{18}O–^{18}O).

$[Ni^{II}LFe^{II}(EtCN)(\eta^5\text{-}C_5Me_5)]BPh_4$ (**1a**-BPh_4): $[Fe^{II}(MeCN)(CO)_2(\eta^5\text{-}C_5Me_5)]BF_4$ (350 mg, 934 μmol) was dissolved in acetonitrile (100 mL). The resulting solution was slowly evaporated by irradiation with an USHIO Optical ModuleX (Deep UV 500, BA-M500) for 4 h to afford a purple powder. A propionitrile solution (30 mL) of $[Ni^{II}L]$ (286.7 mg, 934 μmol) was added to the purple powder, and the resulting mixture was stirred for 18 h; then, $NaBPh_4$ (477.4 mg, 1.40 mmol) was added. The resulting solution was concentrated under reduced pressure to generate insoluble materials, which were removed by filtration. Slow diffusion of diethyl ether into the filtrate yielded black crystals of **1a**-BPh_4, which were collected by filtration, washed with diethyl ether, and dried in vacuo (34 % yield based on $[Fe^{II}(MeCN)(CO)_2(\eta^5\text{-}C_5Me_5)]BF_4$). ^{1}H NMR (300 MHz, [D5]propionitrile, referenced to TMS, 25 °C): $\delta = 1.33$–1.37 (t, 6H, NCH_2CH_3), 1.49 (s, 15H, $C_5(CH_3)_5$), 1.55–1.70, 1.83–1.91, 2.10–2.16, 2.41–2.64, 2.78–2.87 (m, 18H, CH_2), 6.80–6.85, 6.94–6.99, 7.21–7.28 ppm ($B(C_6H_5)_4$). ESI-MS (in propionitrile): *m*/*z* 497.1 ($[\mathbf{1a}\text{-}EtCN]^+$, $I = 100$ % in the range of *m*/*z* 100–2000). FT-IR (KBr disk): 2220 (C≡N), 2850–3050 cm^{-1} (aliphatic C–H). Mössbauer (solid sample at 5 K in the absence of a magnetic field): $\delta = 0.55$, $\Delta E_Q = 2.1$. Elemental analysis calcd [%] for **1a**-BPh_4 ($C_{48}H_{64}BFeN_3NiS_2$): C 66.08, H 7.39, N 4.82; found: C 65.86, H 7.42, N 4.83.

$[Ni^{II}LFe^{II}(MeCN)(\eta^5\text{-}C_5Me_5)]BF_4$ (**1b**-BF_4): $[Fe^{II}(MeCN)(CO)_2(\eta^5\text{-}C_5Me_5)]BF_4$ (326 mg, 870 μmol) was dissolved in acetonitrile (100 mL). The resulting solution was slowly evaporated by irradiation with an USHIO Optical ModuleX (Deep UV 500, BA-M500) for 4 h. The volume of the resulting solution was reduced to 10 mL by evaporation, to which was added an acetonitrile solution (20 mL) of $[Ni^{II}L]$ (267 mg, 869 μmol). After stirring for 18 h, the resulting solution was concentrated under reduced pressure to generate insoluble materials, which were removed by filtration. Slow diffusion of diethyl ether into the filtrate yielded black crystals of **1b**-BF_4, which were collected by filtration, washed with diethyl ether, and dried in vacuo (57 % yield based on $[Fe^{II}(MeCN)(CO)_2(\eta^5\text{-}C_5Me_5)]BF_4$). ^{1}H NMR (300 MHz, [$D_3$]acetonitrile, referenced to TMS, 25 °C): $\delta = 1.36$–1.41 (t, 6H, NCH_2CH_3), 1.50 (s, 15H, $C_5(CH_3)_5$), 1.58–1.75, 1.87–1.96, 2.13–2.25, 2.48–2.69, 2.84–2.96 ppm (m, 18H, CH_2). ESI-MS (in acetonitrile): *m*/*z* 497.1 ($[\mathbf{1b}\text{-}MeCN]^+$, $I = 100$ % in the range of *m*/*z* 100–2000). FT-IR (KBr disk): 2232 (C≡N), 2850–2980 cm^{-1} (aliphatic C–H). Elemental analysis calcd [%] for **1b**-BF_4 ($C_{23}H_{42}BF_4FeN_3NiS_2$): C 44.12, H 6.76, N 6.71; found: C 43.82, H 6.48, N 6.59.

Acknowledgements

This work was supported by Grants-in-Aid [26000008 (Specially Promoted Research), 15H00953, 26410074, and 26810038] from the Ministry of Education, Culture, Sports, Science and Technology (MEXT), Japan and the World Premier International Research Center Initiative (WPI), Japan.

Keywords: dioxygen ligands · hydrogenases · iron · peroxo complexes

How to cite: *Angew. Chem. Int. Ed.* **2016**, *55*, 724–727
Angew. Chem. **2016**, *128*, 734–737

[1] P. Wulff, C. C. Day, F. Sargent, F. A. Armstrong, *Proc. Natl. Acad. Sci. USA* **2014**, *111*, 6606–6611.
[2] J. Fritsch, O. Lenz, B. Friedrich, *Nat. Rev. Microbiol.* **2013**, *11*, 106–114.
[3] W. Lubitz, H. Ogata, O. Rüdiger, E. Reijerse, *Chem. Rev.* **2014**, *114*, 4081–4148.
[4] S. Ogo, K. Ichikawa, T. Kishima, T. Matsumoto, H. Nakai, K. Kusaka, T. Ohhara, *Science* **2013**, *339*, 682–684.
[5] B. C. Manor, T. B. Rauchfuss, *J. Am. Chem. Soc.* **2013**, *135*, 11895–11900.
[6] K. Kim, T. Matsumoto, A. Robertson, H. Nakai, S. Ogo, *Chem. Asian J.* **2012**, *7*, 1394–1400.
[7] S. Ogo, *Chem. Rec.* **2014**, *14*, 397–409.
[8] V. N. Nemykin, R. G. Hadt, *Inorg. Chem.* **2006**, *45*, 8297–8307.
[9] J. P. Collman, R. R. Gagne, C. A. Reed, W. T. Robinson, G. A. Rodley, *Proc. Natl. Acad. Sci. USA* **1974**, *71*, 1326–1329.
[10] J. S. Anderson, A. T. Gallagher, J. A. Mason, T. D. Harris, *J. Am. Chem. Soc.* **2014**, *136*, 16489–16492.
[11] S. E. V. Phillips, *Nature* **1978**, *273*, 247–248.
[12] I. Schlichting, J. Berendzen, K. Chu, A. M. Stock, S. A. Maves, D. E. Benson, R. M. Sweet, D. Ringe, G. A. Petsko, S. G. Sligar, *Science* **2000**, *287*, 1615–1622.
[13] J. Cho, S. Jeon, S. A. Wilson, L. V. Liu, E. A. Kang, J. J. Braymer, M. H. Lim, B. Hedman, K. O. Hodgson, J. S. Valentine, E. I. Solomon, W. Nam, *Nature* **2011**, *478*, 502–505.
[14] S. Hong, K. D. Sutherlin, J. Park, E. Kwon, M. A. Siegler, E. I. Solomon, W. Nam, *Nat. Commun.* **2014**, *5*, 5440.
[15] E. G. Kovaleva, J. D. Lipscomb, *Science* **2007**, *316*, 453–457.
[16] J.-H. Jeoung, M. Bommer, T.-Y. Lin, H. Dobbek, *Proc. Natl. Acad. Sci. USA* **2013**, *110*, 12625–12630.
[17] A. Karlsson, J. V. Parales, R. E. Parales, D. T. Gibson, H. Eklund, S. Ramaswamy, *Science* **2003**, *299*, 1039–1042.

[18] C. J. Cramer, W. B. Tolman, *Acc. Chem. Res.* **2007**, *40*, 601 – 608.
[19] J. Cho, R. Sarangi, J. Annaraj, S. Y. Kim, M. Kubo, T. Ogura, E. I. Solomon, W. Nam, *Nat. Chem.* **2009**, *1*, 568 – 572.
[20] J. Kim, B. Shin, H. Kim, J. Lee, J. Kang, S. Yanagisawa, T. Ogura, H. Masuda, T. Ozawa, J. Cho, *Inorg. Chem.* **2015**, *54*, 6176 – 6183.
[21] O. Pestovsky, S. Stoian, E. L. Bominaar, X. Shan, E. Münck, L. Que, Jr., A. Bakac, *Angew. Chem. Int. Ed.* **2005**, *44*, 6871 – 6874; *Angew. Chem.* **2005**, *117*, 7031 – 7034.

Received: July 29, 2015
Revised: September 28, 2015
Published online: October 28, 2015

